Detection of a nerve agent simulant using single-walled carbon nanotube networks: dimethyl-methyl-phosphonate

2010 Nanotechnology 21 495501

(http://iopscience.iop.org/0957-4484/21/49/495501)

Nanotechnology **21** (2010) 495501 (5pp) doi:10.1088/0957-4484/21/49/495501

Detection of a nerve agent simulant using single-walled carbon nanotube networks: dimethyl-methyl-phosphonate

Yeonju Kim, Seunghyun Lee, Hyang Hee Choi, Jin-Seo Noh and Wooyoung Lee[1]

Department of Materials Science and Engineering, Yonsei University, 262 Seongsanno Seodaemun-gu, Seoul, 120-749, Korea

E-mail: wooyoung@yonsei.ac.kr

Received 7 July 2010, in final form 10 September 2010
Published 16 November 2010
Online at stacks.iop.org/Nano/21/495501

Abstract

Single-walled carbon nanotube (SWNT) networks were used to detect hazardous dimethyl-methyl-phosphonate (DMMP) gas in real time, employing two different metals as electrodes. Random networks of SWNTs were simply obtained by drop-casting a SWNT-containing solution onto a surface-oxidized Si substrate. Although the electrical responses to DMMP at room temperature were reversible for both metals, the Pd-contacting SWNT network sensors exhibited a higher response and a shorter response time than those of the Au-contacting SWNT network sensors at the same DMMP concentration, due to the stronger interactions between the SWNTs and Pd surface atoms. In Pd-contacting SWNT network sensors, the response increased linearly with increasing DMMP concentration and reproducible response curves were obtained for DMMP levels as low as 1 ppm. These results indicate that SWNT networks in contact with Pd electrodes can function as good DMMP sensors at room temperature with scalable and fast response and excellent recovery.

(Some figures in this article are in colour only in the electronic version)

1. Introduction

Dimethyl-methyl-phosphonate (DMMP) is a stimulant for the nerve agent sarin, which is an extremely toxic chemical warfare agent that belongs to the chemical group of organophosphorus compounds [1, 2]. Due to its rapid action and lethality, there is an urgent demand to develop rapid and reliable methods to detect and identify DMMP [3, 4]. Until now, a number of approaches to detect the chemical warfare agent have been reported, using various types of sensors such as semiconducting metal oxide (SMO) sensors [5, 6], microcantilever sensors [7, 8], and surface acoustic wave (SAW) sensors [9–13]. Although these sensors have advantages such as their rapid response and high sensitivity, their operational temperatures are generally high, which limits their wide-spread use.

Carbon nanotubes (CNTs), in particular, single-walled carbon nanotubes (SWNTs) have been intensively investigated as a sensing element for various gases due to their high electrical conductivity, adaptability to surface modulation, interactivity with exterior matters, and the exquisite changeability of their physical properties [14–18]. However, most SWNT-based DMMP sensors have exhibited slow response and long recovery times at room temperature, demonstrating that reproducible, room-temperature sensing of DMMP based on SWNTs is challenging. In this work, we successfully fabricated DMMP sensors using SWNT networks with a proper electrode metal. The sensors operated reversibly and reproducibly at room temperature, and were able to detect infinitesimal amounts of DMMP when Pd electrodes were incorporated. The electrode-dependent DMMP sensing properties of the SWNT network sensors are discussed with regard to the nature of the interactions between SWNTs and electrode surfaces.

[1] Author to whom any correspondence should be addressed.

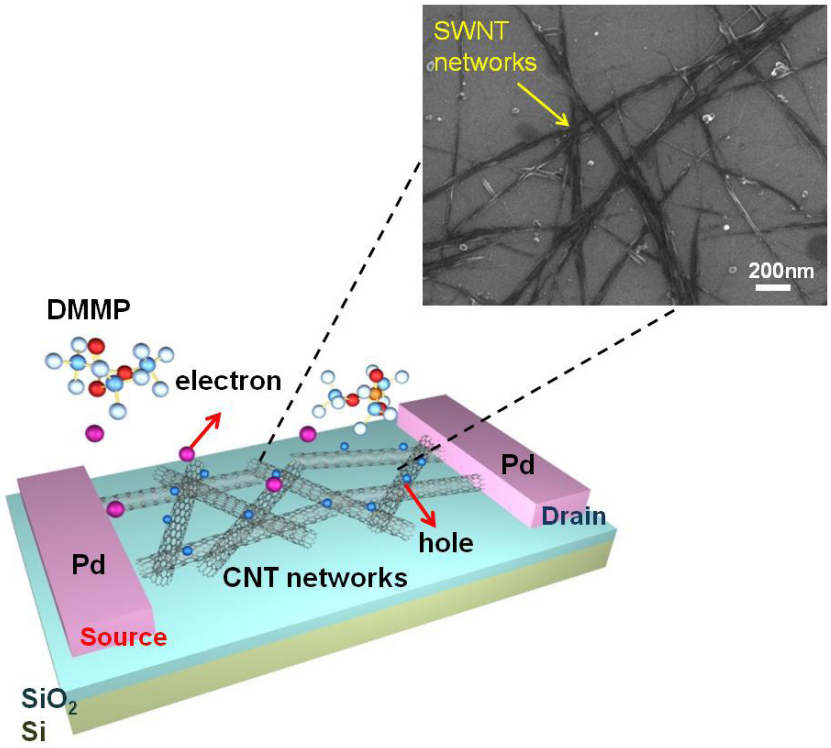

Figure 1. A schematic picture of a SWNT network sensor with Pd electrodes on the oxidized Si substrate. The inset shows a SEM image of the dispersed SWNT networks on the substrate.

2. Experimental details

2.1. Device fabrication

First, we patterned metal electrodes and subsequently dispersed SWNTs on them to avoid the physical damage commonly caused by plasma in conventional post-patterning processes. To fabricate the electrodes, two metals, Pd and Ti/Au, both with thicknesses of 100 nm, were deposited on thermally oxidized Si(100) substrates using ultra-high vacuum (UHV, base pressure: 5×10^{-6} Torr) DC magnetron sputtering. Subsequently, a combination of photolithography and a lift-off process was used to pattern the micron-scale metal electrodes. Then, SWNTs were dispersed between the electrodes by a drop-casting method to produce the SWNT network sensors, as schematically drawn in figure 1. The inset of figure 1 shows a scanning electron microscopy (SEM) image of the dispersed SWNT networks. To improve the dispersion quality of the SWNTs, they underwent a sonication process before drop-casting, as described below.

2.2. Pretreatment of the SWNTs

Purified SWNTs were immersed in a de-ionized water solution containing 0.2 wt% sodium dodecyl sulfate (SDS). The SWNT-containing solution was sonicated for 4 h to ensure good dispersion, followed by vacuum filtration using Teflon filters (pore size: 20 μm). After filtration, the filtered film was rinsed, usually for several minutes, with de-ionized water to remove the SDS surfactant until no bubbles were observed.

To evaluate the quality of prepared SWNTs, we employed Raman scattering, which is one of the most widely used and powerful techniques to characterize CNT samples. Figure 2 shows a Raman spectrum characteristic of our SWNTs. The radial breathing mode of all Raman modes is specifically assigned to the SWNTs, which appears in the high energy region around 1600 cm^{-1} as shown in the figure. Furthermore, a separate examination of the SWNTs by Raman spectroscopy verified a very strong peak at ~1600 cm^{-1} along with a negligible peak at ~1300 cm^{-1}, indicating that our SWNTs were of high quality [19].

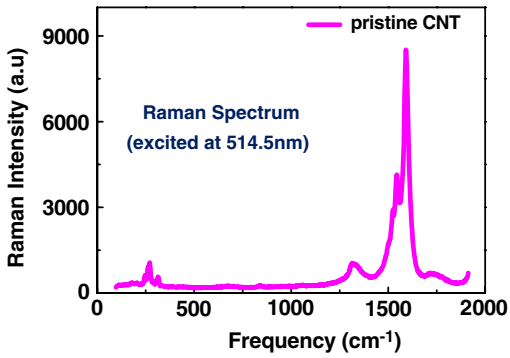

Figure 2. A Raman spectrum of the pretreated single-walled carbon nanotubes.

2.3. Electrical measurements

The measurement system used to evaluate the DMMP sensing properties of the SWNT network sensors consisted of a 180 cc sealed chamber with an inlet and outlet, mass

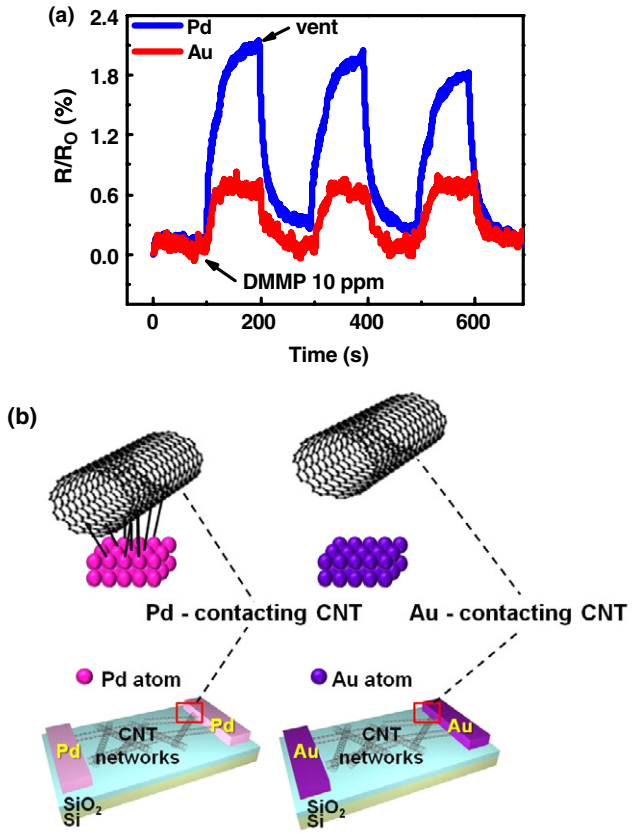

Figure 3. (a) The real-time responses of the SWNT network sensors incorporating Pd and Au electrodes, respectively. The data were obtained at room temperature and the DMMP concentration was 10 ppm for both cases. (b) A schematic representation of the two SWNT/metal contacts.

flow controllers for air and DMMP gas, and digital multimeters connected to a personal computer. The concentration of DMMP was controlled by its pressure relative to the air pressure. The resistance change of the sensor was monitored in real time for 100 s while DMMP gas of the desired concentration was injected into the chamber. Then, the chamber was ventilated for 100 s before undergoing another DMMP injection cycle. All data were acquired using a LabView program through a general-purpose interface bus (GPIB).

3. Results and discussion

The response properties of the SWNT network sensors to DMMP were electrically measured at room temperature employing Pd and Au as electrodes. When a SWNT network sensor is exposed to DMMP, DMMP molecules are adsorbed, transferring electrons to the CNT networks, as shown in figure 1. The injected electrons modulate the carrier density and Fermi level of the semiconducting SWNT networks. The adsorbed DMMP molecules may also deform the local structure of the SWNTs due to their large molecular size, interrupting the free motion of charge carriers. These variations of physical properties result in increases in resistance, as demonstrated in figure 3. Figure 3(a) shows real-time responses of the SWNT network sensors incorporating Pd and Au electrodes, respectively, to 10 ppm DMMP. Here, the response of a SWNT network sensor to DMMP is defined as:

$$\text{Response}(\%) = \frac{\Delta R}{R_O} \times 100(\%) = \frac{R_{\text{DMMP}} - R_{\text{Air}}}{R_{\text{Air}}} \times 100(\%)$$

where R_{DMMP} is the steady state resistance after exposure to DMMP and R_{Air} is the initial resistance before exposure to DMMP. The onsets of the DMMP gas flow and ventilation are indicated by arrows. For both sensors, the response is reversible undergoing DMMP absorption and desorption processes, in the sense that the resistance rapidly decreases when the DMMP is evacuated from the chamber. Comparing the sensors with different electrodes, the Pd-contacting SWNT networks show a cleaner resistance change with a larger response than the Au-contacting networks. For instance, the measured responses are 2.1 and 0.8% at 10 ppm DMMP

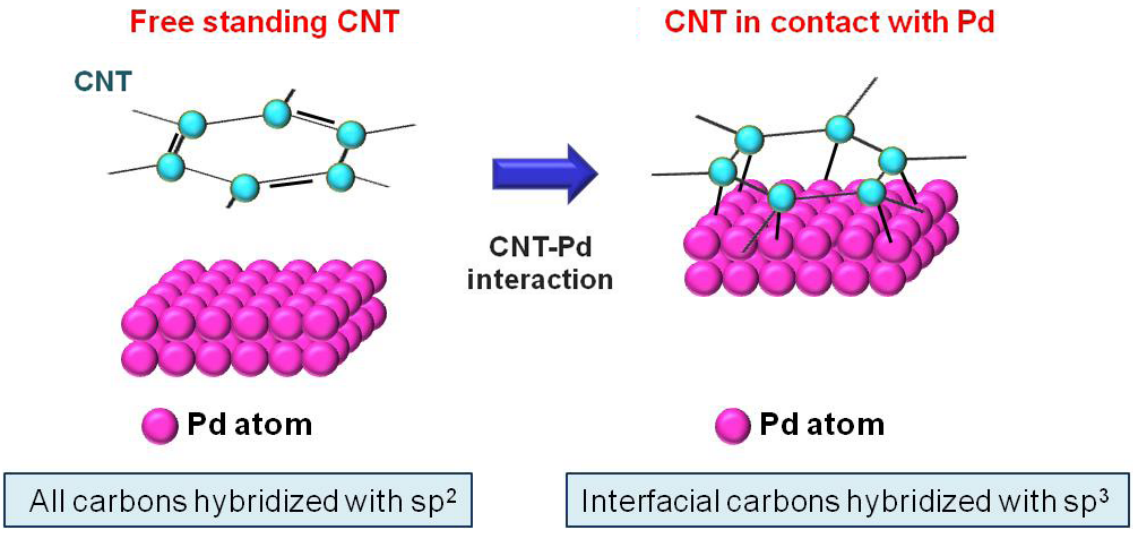

Figure 4. A schematic illustration of the hybridization change of SWNT surface C atoms from sp^2 to sp^3 to form C–Pd bonds at the SWNT/Pd interface.

with the Pd-contacting and Au-contacting SWNT networks, respectively. Despite its larger response, the response and recovery times (15 s) of the Pd-contacting SWNT networks are shorter than those (20 s) of the Au-contacting SWNT networks. Here, the response time is defined as the time required to reach 90% of the total resistance change at a given DMMP gas concentration.

Taking into account that the geometries and constituents are the same for the two sensors except for the electrode materials, the contrast in the response behaviors is expected to originate from the different natures of the SWNT/electrode contacts, as schematically illustrated in figure 3(b). However, it is an oversimplification if the difference is attributed to the different Schottky barrier heights at the two contacts, because Au and Pd have nearly identical work functions (∼5.1 eV). Based on a previous simulation study using the density functional theory (DFT), the atomistic spacing (2.1 Å) between the SWNTs and the Pd surface is shorter than that (3.1 Å) between the SWNTs and the Au surface, due to the stronger interactions of the SWNTs with the Pd surface [20]. Moreover, the stronger interactions of the SWNTs with Pd lead to the more than seven-fold larger binding energy between the carbon (C) atoms and Pd surface atoms, as compared to Au. It is inferred that the larger binding energy between the SWNT and Pd surface is mediated by a hybridization change of Pd-contacting C atoms from sp^2 to sp^3, which involves the breakdown of a weak π bond between two C cores and the formation of another σ-like bond consisting of a lone pair electron of the C atom and an itinerant electron of a Pd surface atom (see figure 4 for schematic illustration). The strong interactions of the SWNTs with Pd and the consequent interfacial bond formation are supported by another simulation study that used first-principles calculations. The simulation revealed that there is no energy barrier to charge transfer between the SWNTs and Pd surface due to the high density of interface states in the original band gap of the SWNTs, resulting from the strong interaction between the nearest C and Pd atoms [21]. The absence of an energy barrier at the SWNTs and Pd contact enables the DMMP-modulated carrier density and mobility to be quickly monitored by measuring the resistance change externally without intensity degradation at the interface, generating a large response and a short response time. This is in contrast to the Au case, where a certain amount of energy barrier should be overcome for carriers to move across the SWNT/Au interface [22].

Owing to the better contact properties, we focused on the Pd-contacting SWNT network sensors for examination of the concentration-dependent electrical responses. Figure 5 shows the real-time responses of the sensor at room temperature as a function of the DMMP concentration. Figure 5(a) displays the original resistance data as a function of time and the responses corresponding to respective DMMP concentrations are shown in figure 5(b), where the responses were converted from the specific concentration segments and overlapped all together. It is clearly seen from these figures that the response gradually decreases with decreasing DMMP concentration. The gradual change of the response is more easily seen in the linear relationship between the response and DMMP concentration,

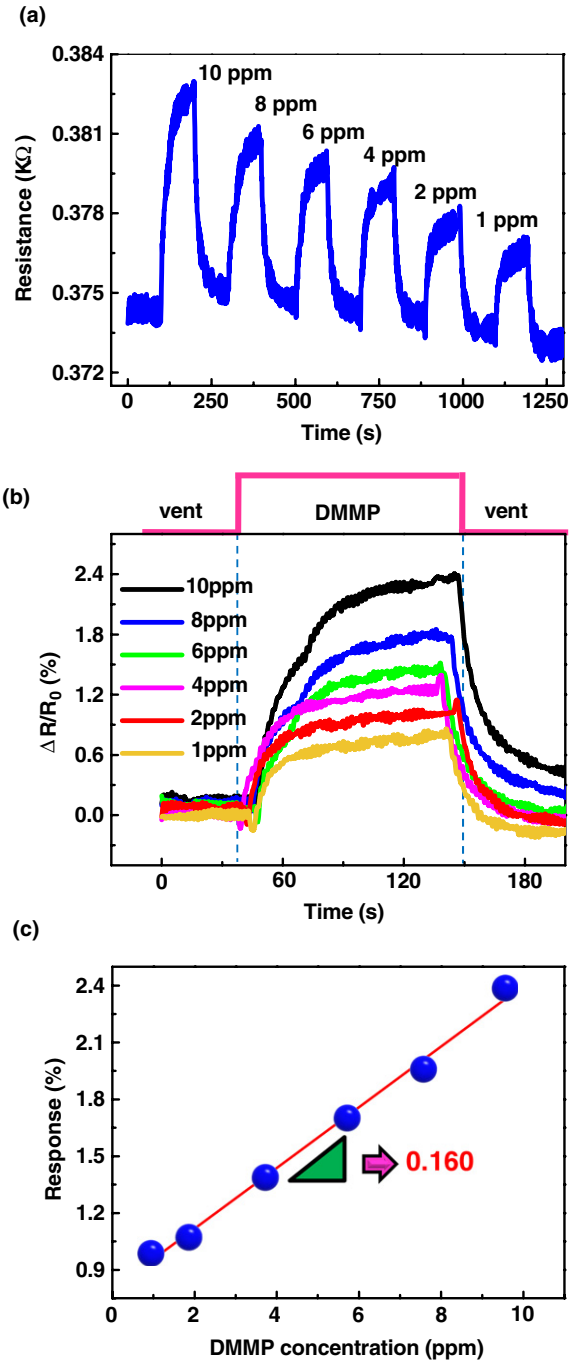

Figure 5. (a) The real-time electrical resistance as a function of DMMP concentration at room temperature and (b) overlapped response curves converted from the data shown in (a) for a Pd-contacting SWNT network sensor. (c) Response versus DMMP concentration plot demonstrating a linear relationship.

as shown in figure 5(c). The linear change of the response with DMMP concentration indicates good functionality and scalable sensitivity of the SWNT network sensor to DMMP, and is ascribed to a DMMP adsorption frequency proportional to its concentration. More specifically, more electrons donated by adsorbed DMMP molecules recombine with holes, which are majority carriers in our p-type SWNTs, increasing the resistance of the sensor by reducing the majority carrier

density along with more scattering chances at higher DMMP concentrations. It is noteworthy that the response curve is still clean and reproducible at 1 ppm DMMP (response ≈0.8). To our knowledge, this is the lowest detection level of DMMP in air ever reported, using pure CNTs without any chemical pretreatment. The small slope (0.160) of the response versus DMMP concentration in figure 5(c) suggests the possibility of detecting even lower concentrations of DMMP, which was partly verified from another experiment in association with this study. This is possible because the high density semiconducting CNT networks are incorporated into the sensor and the CNT/Pd contacts are almost perfect.

4. Conclusions

In summary, we investigated the response behaviors of SWNT network sensors to DMMP gas at room temperature. Two different materials (Pd and Au) were incorporated as electrodes. Although all SWNT network sensors with the different electrodes worked reversibly, the Pd-contacting sensors showed a larger response and a shorter response time at a given DMMP concentration, as compared to the Au-contacting sensors. This was attributed to the barrier-free almost perfect SWNT/Pd contacts originating from the strong interactions between the SWNTs and Pd surface atoms. The Pd-contacting SWNT network sensors exhibited a linear relationship between the response and DMMP concentration as well as a very low detection limit of 1 ppm, making them suitable for DMMP gas sensing. Our results indicate that CNTs with the proper choice of electrode materials can be practically utilized as efficient gas sensing materials.

Acknowledgments

This work was supported by the Agency for Defense Development through the Defense Nano Technology Application Center and Priority Research Centers Program (2009-0093823) through the National Research Foundation of Korea (NRF).

References

[1] Szinicz L 2005 *Toxicology* **214** 167–81
[2] Tomchenko A A, Harmer G P and Marquis B T 2005 *Sensors Actuators* B **108** 41–55
[3] Worek F, Koller M, Thiermann H and Szinicz L 2005 *Toxicology* **214** 182–9
[4] Choi N J, Lee Y S, Kwak J H A, Park J S, Park K B, Shin K S, Park H D, Kim J C, Huh J S and Lee D D 2005 *Sensors Actuators* B **108** 177–83
[5] Kanan S M, Waghe A, Jensen B L and Tripp C P 2007 *Talanta* **72** 401–7
[6] Meier D C, Taylor C J, Cavicchi R E, White E, Ellzy V M W, Sumpter K B and Semancik S 2005 *IEEE Sensors J.* **5** 712–24
[7] Yang Y, Ji H and Fand Thundat T 2003 *J. Am. Chem. Soc.* **125** 1124–5
[8] Karnati C, Du H W, Ji H F, Xu X H, Lvov Y, Mulchandani A, Mulchandani P and ChenW 2007 *Biosens. Bioelectron.* **22** 2636–42
[9] Thomas R C, Yang H C, DiRubio C R, Ricco A J and Crooks R M 1996 *Langmuir* **12** 2239–46
[10] McGill R A, Nguyen V K, Chung R, Shaffer R E, DiLella D, Stepnowski J L, Mlsna T E, Venezky D L and Dominguez D 2000 *Sensors Actuators* B **65** 10–3
[11] Dominguez D D, Chung R, Nguyen V and Tevault R A 1998 *Sensors Actuators* B **53** 186–90
[12] Milner G M 2005 *Proc. SPIE* **5778** 305–16
[13] Zimmermann C, Mazein P, Rebiere D, D'ejous C, Pistr'e J and Planade R 2004 *IEEE Sensors J.* **4** 479–88
[14] Kong J, Franklin N R, Zhou C, Chapline M G, Peng S, Cho K and Dai H 2000 *Science* **287** 622
[15] Novak J P, Snow E S, Houser E J, Park D, Stepnowosreki J L and McGill R A 2003 *Appl. Phys. Lett.* **83** 4026
[16] Snow E S, Perkins F K, Houser S C, Badescu S C and Reinecke T L 2005 *Science* **307** 1942
[17] Zhao J, Buldum A, Han J and Lu J P 2002 *Nanotechnology* **13** 195–200
[18] Cantalini C, Valentini L, Armentano I, Kenny J M, Lozzi L and Santucci S 2004 *Diamond Relat. Mater.* **13** 1301–5
[19] Lee C Y, Baik S, Zhang J, Masel R I and Strano M S 2006 *J. Phys. Chem.* B **110** 11055–61
[20] Maiti A and Ricca A 2004 *Chem. Phys. Lett.* **395** 7–11
[21] Zhu W and Kaxiras E 2006 *Nano Lett.* **6** 1415–9
[22] Shan B and Cho K J 2004 *Phys. Rev.* B **70** 233405